


SCIENTIFIC REPORTS



OPEN

CO₂ production, dissolution and pressure dynamics during silage production: multi-sensor-based insight into parameter interactions

Menghua Li¹, Guilin Shan¹, Haiyang Zhou¹, Wolfgang Buescher², Christian Maack², Kerstin H. Jungbluth², André Lipski³, David A. Grantz⁴, Youheng Fan¹, Daokun Ma¹, Zhongyi Wang¹ , Qiang Cheng¹ & Yurui Sun¹

Silage is a critical global feedstock, but is prone to aerobic deterioration. The dominant mechanism of O₂ transport into silage remains unresolved. Here, multiple sensors tracked O₂ and CO₂, gas pressure (ΔP) between internal silage and ambient air, pH and silage temperature (T_{si}) during the ensilage of maize and ryegrass. We report the first observation that CO₂ produced from microbial respiration was partially dissolved in silage water, with evidence of negative or positive ΔP depending on the changing balance between CO₂ production and dissolution. The $\Delta P < 0$ reflected an apparent respiratory quotient (RQ) < 1 . Net CO₂ production was much greater in anaerobic fermentation stage than in initial aerobic phase or later aerobic feed-out phase. O₂ transport into silage is intimately linked to the dynamics of net CO₂, ΔP , microbial activity, pH and T_{si} . These results suggested that both gas diffusion (based on Fick's law) and advective transfer (Darcy's law) play equally important roles in governing the complex temporal progression of inward and outward gas fluxes to and from the silage interior. Even though low pH suppressed microbial activity and supported aerobic stability, the negative ΔP increased the risk of O₂ entry and aerobic deterioration during feed-out phase.

Silage is an important preservation technique, used world-wide to provide a nutritious and palatable animal feed months after harvest¹. It is estimated that 200 million tons of dry matter (DM) are ensiled worldwide annually^{1,2}. A significant fraction of the nutritive value is lost due to biological oxidation.

The biochemical production of silage relies on lactic acid anaerobic fermentation. The silage-making process is generally divided into four temporal phases: an initial aerobic phase, a fermentation phase, a prolonged storage phase, and a final feed-out phase³. The fermentation and storage phases are dominated by anaerobic processes. As a result, silage is susceptible to oxidation because it contains aerobic bacteria, yeasts and molds (fungi) that are dormant under anaerobic conditions. Introduction of oxygen (O₂) enables these aerobic microorganisms to be quickly activated, producing carbon dioxide (CO₂) and water through aerobic respiration³⁻⁵ and inducing loss of dry matter and nutrients, i.e. "spoilage" of the silage^{3,6,7}. During feed-out, when the silo is opened for feeding to livestock, the face of the silage is unavoidably exposed to the oxidizing atmosphere and aerobic losses can be substantial³.

The amount of O₂ present within the silage is affected by numerous competing factors, including silage density or porosity, moisture content, wind velocity and direction, thermal buoyancy and gradients in gas concentration, density and pressure^{4,8,9}. Two physical mechanisms of O₂ transport to the silage interior during ensilage and storage have been identified as gas diffusion, which is governed by the concentration gradient between the silage pore space and ambient air, and advective transfer, driven by differential gas pressure ($\Delta P = P_{air} - P_{silage}$) across the

¹College of Information and Electrical Engineering, China Agricultural University, Key Lab of Agricultural Information Acquisition Technology, Ministry of Agriculture, 100083, Beijing, China. ²Department of Agricultural Engineering, The University of Bonn, 53115, Bonn, Germany. ³Institute of Nutrition and Food Science, The University of Bonn, 53115, Bonn, Germany. ⁴Department of Botany & Plant Sciences, University of California at Riverside, Kearney Agricultural Center, Parlier, CA, 93648, United States. Menghua Li, Guilin Shan and Yurui Sun contributed equally to this work. Correspondence and requests for materials should be addressed to Q.C. (email: chengqiang@cau.edu.cn) or Y.S. (email: pal@cau.edu.cn)



Figure 1. The experimental test silo for both Test-A and Test-B, which included ① CO₂ sensor ② O₂ sensor ③ temperature sensor ④ pH sensor, ⑤ ALMEMO data-logger ⑥ air-tight cylinder and ⑦ test substrate (here fresh chopped maize).

bunker silo seals. The first may be modelled based on Fick's law^{4,8,10–14}, and the second based on Darcy's law^{15–18}. Despite this mathematical tractability, the dominant mechanism for transport of O₂ into the silage remains in question⁷.

While the biochemical process of silage-making has been mostly characterized, determination of conditions within the developing silage has been challenging. For gas composition and concentration inside the silage, a common method has been to extract gas samples from the silage for later analysis using a laboratory gas chromatograph^{8,18,19}. Despite sufficient accuracy of the gas chromatography method, two technical issues are encountered. First, sample extraction may result in additional O₂ entering the silage. Second, the method is time consuming and thus unable to track the dynamics of silage gasses. Measurement of pH within the silage during its solid-state fermentation has also been difficult to achieve²⁰.

Despite these challenges, obtaining and characterizing these process level data will contribute to understanding and improving silage yield and quality. Here we present the first multi-sensor-based, simultaneous measurements of internal O₂, CO₂, ΔP , pH, and internal silage temperature (T_{si}) over the whole silage-making process. The major objective of this study was to reveal the previously unknown dynamic interactions of the key parameters governing silage development and quality.

Results

Fresh plant materials (Test-A). A unique suite of sensors was placed in a test silo (Fig. 1) such that naturally occurring changes could be monitored under realistic gas-tight conditions. Details are presented in Methods (below). The testing period consisted of the initial aerobic phase (about 3 h) and the anaerobic fermentation period (about 100 h), repeated three times with each of two fresh materials (maize and ryegrass).

The time courses of O₂, CO₂, pH, ΔP and T_{si} (three independent replicates; Test-A) and relationships between ΔP and CO₂ in Test-A were obtained from fresh-chopped maize (Fig. 2a,c) and fresh ryegrass (Fig. 2b,d). During the aerobic period, the initial pH was 5.8 for maize and 6.1 for ryegrass (Table 1; Fig. 2a,b), which was conducive to high activity of microorganisms and plant proteolytic enzymes^{5,8,18,21}. While O₂ was rapidly depleted to near zero in each test silo, the increase in CO₂ was minimal.

Most of the CO₂ was produced during the anaerobic period, rather than the aerobic period. During the anaerobic phase, O₂ remained depleted, but CO₂ increased 3- to 5-fold, accompanied by a pronounced decline of pH (maize to pH 4.6 and ryegrass to pH 5.2). The decline in pH lagged the depletion of O₂ in both cases (Fig. 2a,b), reflecting increasing anaerobic lactic acid production by lactic acid bacteria (LAB)²².

The rate of CO₂ production was linearly related to pH for both fresh maize (Fig. 3a, $R^2 = 0.8902$, $p = 6.04 \times 10^{-30}$), and fresh ryegrass (Fig. 3b, $R^2 = 0.7638$, $p = 6.04 \times 10^{-40}$). When pH declined to 4.6 in maize and 5.2 in ryegrass, CO₂ production and further changes in pH and ΔP were greatly reduced (Figs 2 and 3). This reflects suppression of microbial activity and further acid production by the reduced pH, despite the modest increase in counts of LAB observed in maize (Table 1), and the substantial increase observed in ryegrass.

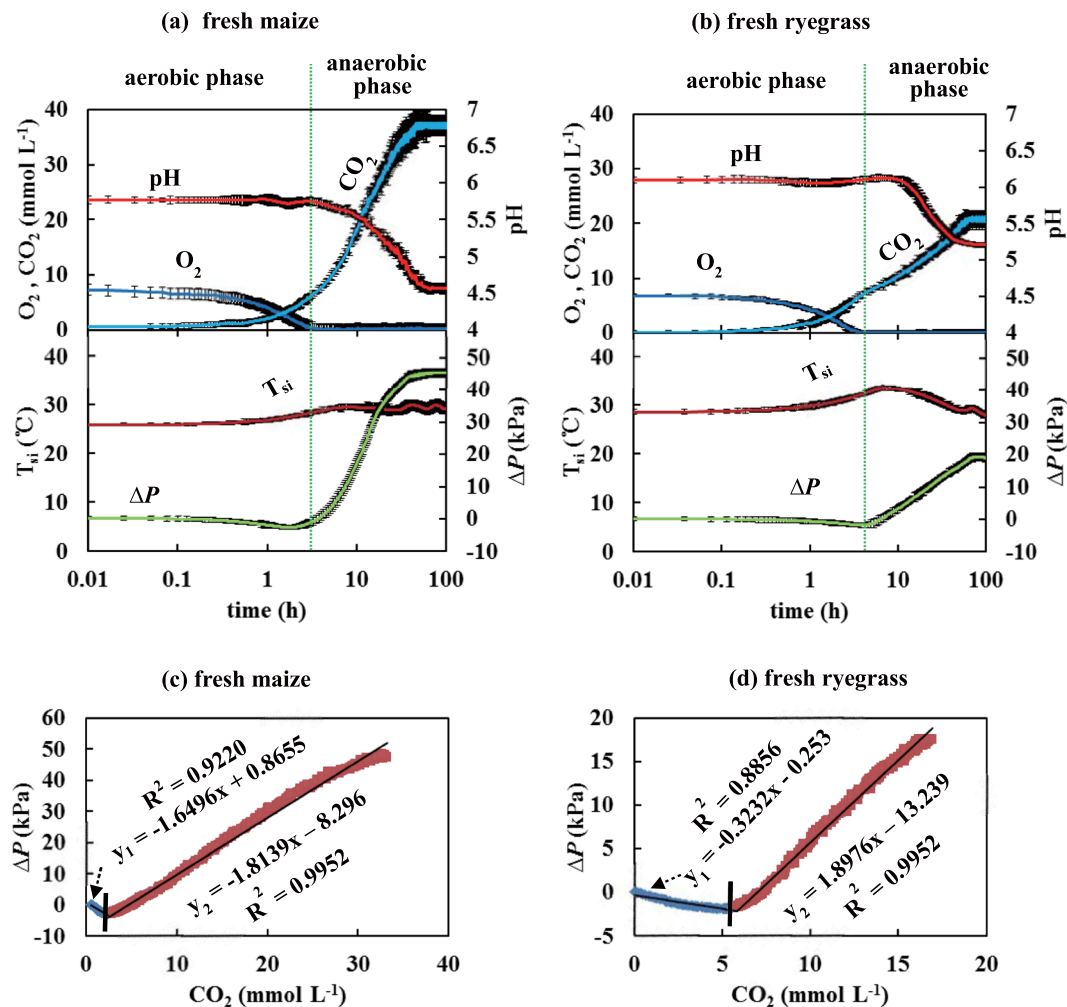


Figure 2. The time courses (means \pm s.e.) of O₂ and CO₂ concentrations, pH, ΔP (inside to ambient) and internal silage temperature, T_{si}, during Test-A, the ensilage of fresh-chopped maize (Fig. 2a) and fresh-cut ryegrass (Fig. 2b). Note the logarithmic time axis. The relationships between ΔP and CO₂ shown as piecewise linear regressions in Test-A during ensilage of fresh maize (Fig. 2c) ($R^2 = 0.9220$, $p = 5.94 \times 10^{-40}$; $R^2 = 0.9952$, $p = 7.12 \times 10^{-80}$), and fresh ryegrass (Fig. 2d) ($R^2 = 0.8856$, $p = 3.57 \times 10^{-61}$; $R^2 = 0.9952$, $p = 3.70 \times 10^{-90}$) in Test-A.

| | | Fresh BD (kg m ⁻³) | DMC (%) | pH | Lactic-acid bacteria (colony forming units; Cfug ⁻¹) | Yeasts (Cfu g ⁻¹) | Molds (Cfu g ⁻¹) | Total-bacteria (Cfu g ⁻¹) |
|------------------|---------|--------------------------------|---------|-----|--|-------------------------------|------------------------------|---------------------------------------|
| Fresh maize | initial | 625 | 27 | 5.8 | $1.9(0.2) \times 10^8$ | $1.2(0.1) \times 10^5$ | ND | $1.9(0.3) \times 10^8$ |
| | end | | | 4.6 | $4.5(0.9) \times 10^8$ | $5.6(1.8) \times 10^5$ | ND | $2.1(1.3) \times 10^8$ |
| Fresh ryegrass | initial | 425 | 45 | 6.1 | $3.0(1.7) \times 10^5$ | $5.1(3.9) \times 10^5$ | $2.2(0.7) \times 10^6$ | $2.6(0.4) \times 10^8$ |
| | end | | | 5.2 | $3.8(0.4) \times 10^8$ | $1.6(0.5) \times 10^5$ | $3.9(4.4) \times 10^5$ | $1.4(0.2) \times 10^8$ |
| Ensiled maize | initial | 625 | 35 | 4.0 | $2.5(1.3) \times 10^9$ | $2.3(3.7) \times 10^6$ | ND | $1.6(0.3) \times 10^9$ |
| | end | | | 3.9 | $2.9(2.6) \times 10^7$ | $6.8(7.5) \times 10^4$ | $>1.0 \times 10^3$ | $2.6(3.7) \times 10^8$ |
| Ensiled ryegrass | initial | 425 | 43 | 5.2 | $3.0(0.2) \times 10^6$ | ND | ND | $3.9(0.8) \times 10^6$ |
| | end | | | 5.1 | $2.7(1.9) \times 10^6$ | ND | ND | $6.0(2.8) \times 10^6$ |

Table 1. Physical properties, pH and counts of microorganisms of the tested materials. Values marked ND are below the level of detection.

ΔP exhibited a modest initial decline to a negative peak of -2.6 kPa in maize and -1.8 kPa in ryegrass, followed by a large increase to $+45.4$ kPa in maize and $+19.1$ kPa in ryegrass (Fig. 2a,b). Reasoning from the ideal gas law, observations of $\Delta P < 0$ could result either from a loss of mass in the gas phase or from a decline in T_{si}, or a combination of both. Similarly, $\Delta P > 0$ could result from an increase of gas phase mass and/or elevation of T_{si}. The increase in ΔP beginning as O₂ declined to near zero (Fig. 2a,b) closely tracked the time course of rising

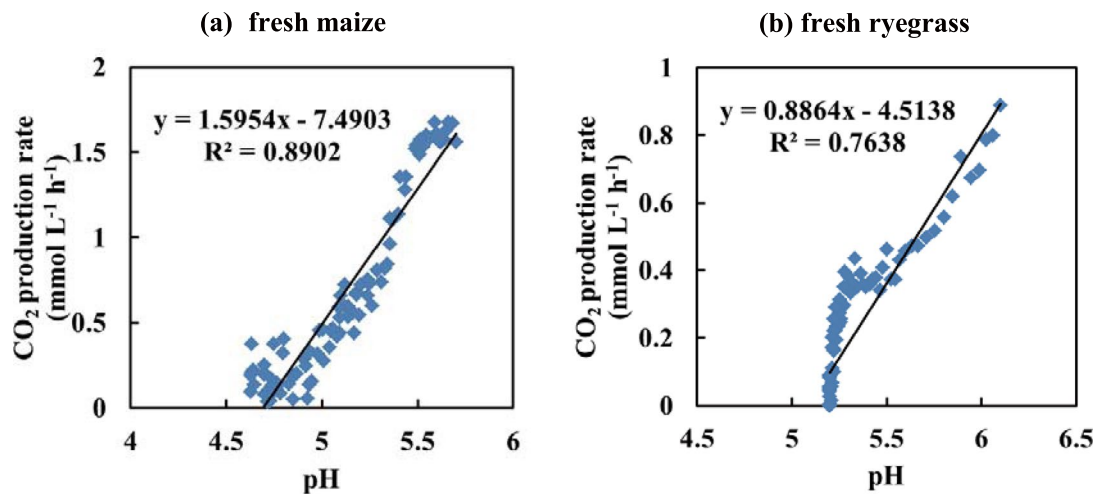


Figure 3. Correlation between pH and the rates of CO₂ production during the anaerobic phase. Points represent hourly averages for (a) fresh maize ($R^2 = 0.8902$, $p = 6.04 \times 10^{-30}$) and (b) fresh ryegrass ($R^2 = 0.7638$, $p = 5.60 \times 10^{-40}$).

CO₂ in each test silo, demonstrating the essential role of gas phase CO₂ production exceeding O₂ consumption (Fig. 2a,b; upper panels). The CO₂ produced in the fresh maize system was considerably greater than that in the fresh ryegrass, reflected in both CO₂ and ΔP (Fig. 2a,b).

The relationship between CO₂ and ΔP was biphasic in both systems (Fig. 2c,d). Piecewise regression analysis revealed strong linear relationships in both phases for maize (Fig. 2c; $R^2 = 0.9220$, $p = 5.94 \times 10^{-40}$ for y_1 and $R^2 = 0.9952$, $p = 7.12 \times 10^{-80}$ for y_2) and for ryegrass (Fig. 2d; $R^2 = 0.8856$, $p = 3.57 \times 10^{-61}$ for y_1 and $R^2 = 0.9952$, $p = 3.70 \times 10^{-90}$ for y_2).

An increase in T_{si} was observed in both systems during the aerobic phase (Fig. 2a,b). This stabilized at an elevated level in maize, but declined to original values in ryegrass during the anaerobic phase. More heat was generated during aerobic than during anaerobic respiration^{8,23}. At the end of the ensiling process (about 100 h), pH was low, ΔP was elevated, and all parameters were stable. The experimental system remained anoxic.

Ensiled plant materials (Test-B). The time courses of O₂, CO₂, pH, ΔP and T_{si} and relationships between ΔP and CO₂ in Test-B were obtained with three repetitions (Fig. 4). The aerobic period for ryegrass was longer than for maize. This may be partially attributed to the lower packing density and resulting greater porosity in the ensiled ryegrass, leading to more O₂ molecules entrapped but fewer microorganisms within the test silo⁹. The initial populations of LAB in ensiled ryegrass (10^6 Cf u g⁻¹) and total-bacteria (10^6 Cf u g⁻¹) were significantly lower than in ensiled maize (10^9 Cf u g⁻¹ and 10^9 Cf u g⁻¹, respectively; Table 1). Molds were initially below detection threshold (10^2 Cf u g⁻¹) in maize, while both yeasts and molds were below detection threshold (10^2 Cf u g⁻¹) in ryegrass throughout the experiment (Table 1). The fresh maize and the ensiled maize had similar (10^8 Cf u g⁻¹) microbial populations, whereas the fresh ryegrass had higher (10^8 Cf u g⁻¹) populations than the ensiled ryegrass (10^6 Cf u g⁻¹; Table 1).

In contrast to the biphasic time courses observed in Test-A (cf. Fig. 2), the CO₂ concentration in both ensiled materials was lower than in the same material in the fresh state (cf. Figs 2 and 4) and ΔP only exhibited negative values throughout Test-B. The CO₂ concentration in the ensiled ryegrass was greater than in the ensiled maize (Fig. 4), even though the microbial counts in the ensiled ryegrass were lower (Table 1). As a result, the decline to negative ΔP in the ensiled maize was greater than the ensiled ryegrass.

As with the fresh material, observations of $\Delta P < 0$ reflected a decline in gas phase mass inside the test silo. The simultaneous measurements of O₂ and CO₂ over time indicate that the respiratory quotient (RQ, ratio of mole CO₂ evolution per mole O₂ uptake²⁴), was significantly below 1.0 for both ensiled materials (Fig. 5a,b; blue line). While aerobic carbohydrate metabolism exhibits a theoretical RQ = 1.0, i.e. 1 mole of CO₂ evolved per 1 mole of O₂ consumed^{5,25}, in Test-B the observed RQ < 1.0 suggested the concurrence of CO₂ production by aerobic respiration and simultaneous partial CO₂ dissolution in interstitial silage water. This process was dominated by CO₂ dynamics since the solubility of CO₂ in H₂O (39.2 mmol L⁻¹ at 20 °C) is much greater than that of O₂ (1.38 mmol L⁻¹)²⁶.

The relatively low CO₂ concentrations in both ensiled substrates are likely to reflect several interacting factors. First, the produced CO₂ was partially dissolved in the interstitial silage water. Second, after the fermentation (anaerobic phase), the residual plant sugar in the ensiled materials was sufficiently low that the CO₂ produced from microbial respiration was minimal. In addition, microbial metabolic activity was further depressed by low pH^{5,8,18,21}. The greater CO₂ in ensiled ryegrass than ensiled maize reflects the lower density and mass of silage, greater porosity and volume of O₂ entrapped, despite the similar O₂ concentrations, and less available silage water for gas dissolution. Therefore, more CO₂ was produced through aerobic respiration and less CO₂ was dissolved in the interstitial silage water.

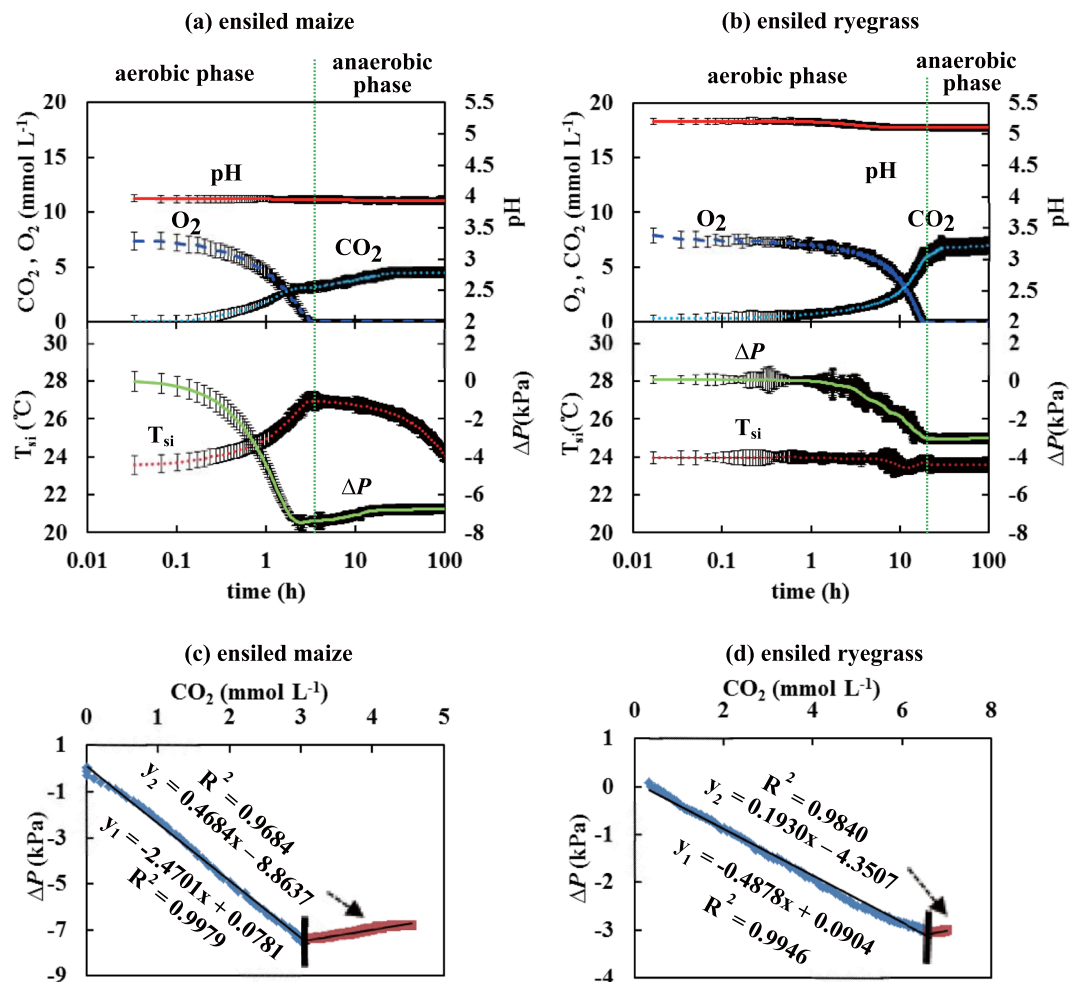


Figure 4. The time courses (means \pm s.e.) of O₂, CO₂, pH, ΔP and T_{si} observed in the re-ensiled maize (Fig. 4a) and the re-ensiled ryegrass (Fig. 4b) during Test-B. The relationships between ΔP and CO₂ shown as piecewise linear regressions during re-ensilage of fresh maize (Fig. 4c) (R² = 0.9979, $p = 3.30 \times 10^{-94}$, R² = 0.9684, $p = 4.21 \times 10^{-87}$) and re-ensiled ryegrass (Fig. 4d) (R² = 0.9946, $p = 6.90 \times 10^{-86}$, R² = 0.9840, $p = 8.9 \times 10^{-89}$) in Test-B.

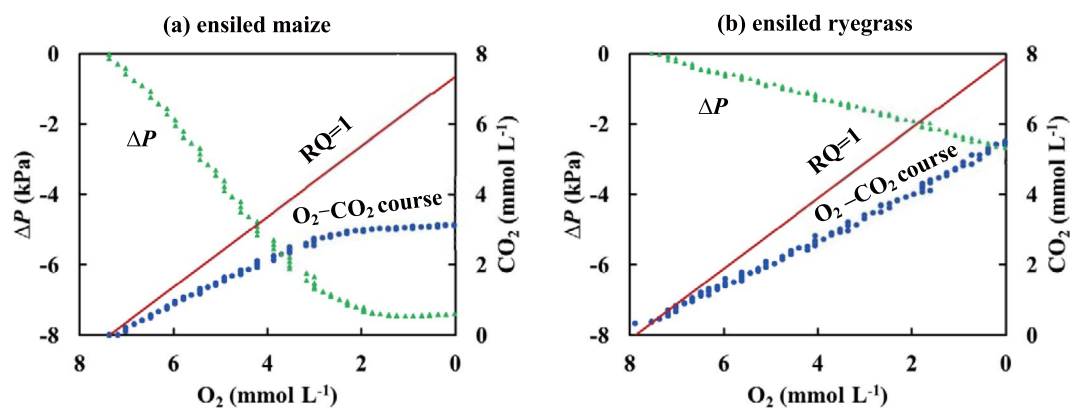


Figure 5. The apparent respiratory quotient (RQ) determined from the simultaneous measurements of O₂ and CO₂ for the re-ensiled maize (Fig. 5a) and for the re-ensiled ryegrass (Fig. 5b) during Test-B (aerobic phase). The reference line of RQ = 1 is the expected value from carbohydrate metabolism. The O₂-CO₂ course below RQ = 1 (i.e. actual RQ < 1) in Fig. 5a or Fig. 5b reflects the CO₂ not detected by the sensor and apparently dissolved in the aqueous phase. Note the declining axes for O₂.

As observed for fresh material (cf. Fig. 2c,d), strong biphasic linear relationships were observed by piecewise regression between ΔP and CO_2 in both ensiled maize (Fig. 4c: $R^2 = 0.9979$, $p = 3.30 \times 10^{-94}$ for y_1 and $R^2 = 0.9684$, $p = 4.21 \times 10^{-87}$ for y_2) and ensiled ryegrass (Fig. 4d: $R^2 = 0.9946$, $p = 6.90 \times 10^{-86}$ for y_1 and $R^2 = 0.9840$, $p = 8.9 \times 10^{-89}$ for y_2). In both fresh and ensiled materials, the goodness of fit demonstrated that ΔP varied primarily with CO_2 , rather than with T_{si} .

Discussion

In Test-A, $\Delta P < 0$ was observed over a quite short period (around 5 h) following introduction of fresh plant material. The transition of ΔP from negative to positive indicated that the CO_2 produced by microbial respiration rapidly exceeded the capacity for CO_2 dissolution, while high pH allowed sustained metabolic activity during the early stages of ensilage. Therefore, ΔP is a potentially useful indicator not only of CO_2 dynamics, but also of microbial activity. On the other hand, the solubility of CO_2 in H_2O is a function of numerous interacting factors, including pH, partial pressure of CO_2 (Henry's law), ambient temperature (van't Hoff equation), interaction between internal gas pressure and temperature (the ideal gas law), sugar content in water and water content in the substrate^{26–30}. Adding further complexity, dissolution of CO_2 in water is exothermic²⁷, contributing to the observed increases in both T_{si} and ΔP . Since dissolution of CO_2 in water is the outcome of the chemical reaction, $\text{CO}_2 + \text{H}_2\text{O} \leftrightarrow \text{H}_2\text{CO}_3$ ²⁶, the decline of silage pH over the silage-making process resulted not only from the anaerobic fermentation of plant sugars such as glucose and fructose to lactic acid by LAB, but also from the dissolution of CO_2 in water. As a result, the time courses of net CO_2 production and ΔP are not readily simulated using current methods. Here we characterize the trajectory of variation in ΔP ($\Delta P = 0$) \rightarrow ($\Delta P < 0$) \rightarrow ($\Delta P > 0$) \rightarrow ($\Delta P < 0$) throughout the silage production process. Observations of $\Delta P < 0$ indicate apparent $\text{RQ} < 1$, reflecting the sequestration of CO_2 , and $\Delta P > 0$ reflects the greater amount of CO_2 produced during anaerobic respiration. While other gases may contribute to these effects, CO_2 dominates because concentrations of H_2 , CH_4 and N_2O in silage are very low compared to N_2 , O_2 , and CO_2 ^{5,18,19,31–33}, and H_2 and N_2 exhibit low solubility in silage water.

For a field-scale bunker silo during feed-out phase, the working face is exposed to air as the silage is unloaded for feeding to livestock. This results in re-ensiling of the remaining material and unavoidable aerobic deterioration in the surface zone as O_2 penetrates into the silage. With the two ensiled plant materials, Test-B provided an analog of these biochemical and physical processes of aerobic respiration and partial dissolution of CO_2 in the interstitial silage water. Here we infer changes in the dissolved CO_2 in the silage water, but carefully evaluate the role of gas phase advective transfer associated with CO_2 dissolution. Our unique sensor combination allowed us to follow O_2 and CO_2 , *in situ*, while tracking the variations of ΔP and T_{si} simultaneously, with ΔP employed as an indicator of the net CO_2 dynamics based on the ideal gas law. For this reason, Test-B was conducted under gas-tight and constant volume conditions. Most real-world silage-making processes, including the maize bunker silo and ryegrass bale system used here, rarely exhibit this level of seal^{5,17,34}. Our experimental design revealed the substantial and contrasting levels of ΔP generated by two common plant materials at the early ensiling stage and in the ensiled state. The rigorous vacuum sealing of our test silos allowed ΔP to vary over a range of -7.5 to $+45.4$ kPa for maize and of -3.1 to 19.1 kPa for ryegrass.

To our knowledge, we provide the first evidence of the physical and chemical interactions involved in the production of CO_2 , its partial dissolution in silage water, and resulting negative and positive pressures, depending on stage of ensilage. The $\Delta P > 0$ ('balloon') phenomenon has been reported previously^{17–19,35}. One study¹⁹ observed an increase in O_2 and N_2 but a decrease in CO_2 , measured at the end of the eight-day fermentation phase, and inferred a reversal of gas movement from efflux to influx, as a result of the reversal of ΔP from positive to negative. However, fundamental processes and causative factors were not explored. Our multi-sensor measurements provide insight into these parameters with essential interactions and dynamics, and the resulting relationships between net CO_2 production, O_2 consumption, and variations in ΔP , pH and T_{si} .

Conclusions

In situ tracking of O_2 depletion, CO_2 production and dissolution, pH lowering-processes and ΔP dynamics has been realized during early and late phases of silage production, using multi-sensor techniques. CO_2 production was much greater from anaerobic than aerobic processes. The ΔP exhibited both positive and negative values, indicative of net values of CO_2 production and dissolution. For the two common silage materials tested here, the resulting ΔP is of the order of tens of kPa. Since the negative ΔP allowed more O_2 entry through the silo face, risk of aerobic deterioration in the feed-out phase could be potentially higher than anticipated. These interactions are diagnostic of the previously unknown behavior during ensilage and re-ensiling processes. These results suggest that both gas diffusive and advective transfer play equally important roles in governing the complex temporal progression of inward and outward gas fluxes to and from the silage interior. Future efforts to develop simulation of the ensilage process should incorporate both Fick's law and Darcy's law. The fusion of our data with improved process models will support development of improved silage management.

Methods

General information on the sensors used. Table 2 lists general information of all sensors used for this study. These sensors employ different principles, each providing sufficient temporal response (< 1 min.) to meet the data sampling requirement. This level of performance is critical for tracking O_2 as it is converted to CO_2 , in order to interpret the resulting ΔP and T_{si} dynamics. Cross calibration of the O_2 and the CO_2 sensors were carried out in advance of the experiment³⁶.

During each test period the pH sensor tip (diameter 2 mm) was enclosed in a small piece of well-wetted porous plastic to improve hygroscopic contact with the test material. The porous plastic was rinsed with deionized water and then dried naturally. Initial pH was determined using a standard protocol for silage³⁷, by extracting 25 g of maize or ryegrass material with 0.225 L deionized water in a glass vessel for 30 min. This provided an

| Parameter | Sensor-Type | Manufacturer | Range/Accuracy | Response (s) | Principle |
|----------------|------------------------|--|--|--------------|---------------------------------|
| Oxygen | KE-50 | FIGARO Engineering Inc. Osaka, Japan | 0–100% (vol.)/ $\pm 2\%$ of full scale (fs) | 60 | Electrochemistry |
| Carbon Dioxide | Prime 3 | Clairair Ltd. Essex, UK | 0–100% (vol.)/ $\pm 3\%$ fs | 60 | NDIR |
| Pressure | FDA612SR | Alborn Mess- und Regelungstechnik GmbH Germany | ± 1000 (mb)/ $\pm 0.5\%$ of final value in range | 1 | Piezo-resistive pressure sensor |
| Temperature | FTA15 NiCr-Ni ZA9020FS | Alborn Mess- und Regelungstechnik GmbH Germany | -40 – 160 ($^{\circ}\text{C}$)/ ± 0.1 $^{\circ}\text{C}$ | 2 | Thermocouple |
| pH | BlueLine 21 Ph | Alborn Mess- und Regelungstechnik GmbH Germany | 2 – 13 / ± 0.3 | < 60 | Potentiometric analysis |

Table 2. Sensor specifications.

initial reference value for comparison with the initial value of the inserted pH sensor when encased in the porous plastic wetted with the same solution. In addition, the pH sensor was repeatedly calibrated against three buffer pH-solutions (ZB98PHPL4, pH = 4.0, ZB98PHPL7, pH = 7.0, and ZB98PHPL10, pH = 10.0; AHLBORN GmbH, Germany) at 20 $^{\circ}\text{C}$ prior to and after the experiment.

Experimental test silo. Two PVC cylinders (inner diameter: 370 mm, height: 600 mm, wall thickness: 15 mm) together with a lid (diameter 400 mm, thickness 20 mm) were used as the experimental silos (Fig. 1). To make the cylinder gas-tight, a rubber membrane (diameter: 400 mm, thickness: 10 mm) was affixed by a layer of vacuum grease to the inside of the lid, which was secured using six equidistantly-spaced fasteners. Five access ports through the lid and membrane allowed connection of the sensors inside the cylinder to a data logger (ALMEMO-2890-9, 9-channel, AHLBORN GmbH, Germany) placed outside. After each cable was placed through a hole, the space around the cable and all cable terminals were sealed with vacuum grease. The data logger operated at a sampling interval of 3 min throughout the experiment.

Microbial analyses. Thirty grams of silage were suspended in 270 ml of $\frac{1}{4}$ -strength Ringer solution (2.25 g l $^{-1}$ NaCl, 0.105 g l $^{-1}$ KCl, 0.06 g l $^{-1}$ CaCl $_2$, 0.05 g l $^{-1}$ NaHCO $_3$) (Merck, Darmstadt, Germany) and homogenized in a mixer for one minute. From this suspension, total bacterial counts were analyzed on plate-count agar (5.0 g l $^{-1}$ enzymatic digest of casein, 2.5 g l $^{-1}$ yeast extract, 1.0 g l $^{-1}$ glucose, 15 g l $^{-1}$ agar, pH 7.0) (Merck, Darmstadt) after aerobic incubation at 30 $^{\circ}\text{C}$ for 2 days. Lactic acid bacteria (LAB) were quantified from this suspension on de Man, Rogosa and Sharpe (MRS)-agar (10 g l $^{-1}$ enzymatic digest of casein, 10 g l $^{-1}$ meat extract, 4 g l $^{-1}$ yeast extract, 20 g l $^{-1}$ glucose, 2 g l $^{-1}$ K $_2$ HPO $_4$, 1.08 g l $^{-1}$ tween 80, 2 g l $^{-1}$ triammonium citrate, 5 g l $^{-1}$ sodium acetate, 0.2 g l $^{-1}$ MgSO $_4$ \times 7 H $_2$ O, 0.05 g l $^{-1}$ MnSO $_4$ \times 4 H $_2$ O, 14 g l $^{-1}$ agar, pH 5.7) (Merck, Darmstadt). MRS agar plates were incubated anaerobically using an Anaerocult system (Merck, Darmstadt). Yeasts and molds were detected using yeast extract glucose chloramphenicol (YGC)-agar (5.0 g l $^{-1}$ yeast extract, 20.0 g l $^{-1}$ glucose, 0.1 g l $^{-1}$ chloramphenicol, 14.9 g l $^{-1}$ agar, pH 6.6) (Merck, Darmstadt). These agar plates were incubated at 25 $^{\circ}\text{C}$ for 3 days.

Test-A. This was an analogue to the ensiling phase using fresh chopped whole shoots of maize (*Zea mays*) including the cobs (dry matter content, DMC of 27%) and fresh-cut ryegrass (*Lolium perenne*; DMC of 45%). The resulting biomass was finely chopped and packed to high bulk density (BD) in separate cylinders (maize: 625 kg m $^{-3}$, ryegrass, 425 kg m $^{-3}$) using a hydraulic ram (360 mm diameter circular foot), in approximately six layer increments to ensure uniform density. Five holes (diameter 10 mm, depth 100 mm) through the top layer of silage, aligned with the holes in the lid, were drilled using a hole-saw for the installation of O $_2$, CO $_2$, ΔP , pH and T $_{\text{si}}$ sensors.

Test-B. Test-B used previously ensiled maize with DMC of 35% and ryegrass with DMC of 43%. Ensiled maize (harvested and ensiled autumn 2015) was obtained from 20 cm behind the freshly cut silage face in a concrete bunker silo (40 \times 6 \times 3.5 m), located at the Frankenforst research farm (University of Bonn, Germany). Ensiled ryegrass was obtained from a silage bale (harvested and ensiled autumn 2015), which was stored outside, wrapped in four layers of plastic film (thickness: 0.025 mm). The maize and ryegrass silages were re-ensiled in the test silos, and packed with the hydraulic ram to a high BD of 625 kg m $^{-3}$ and 425 kg m $^{-3}$, respectively. The sensors were installed as for the fresh materials. To achieve similar temperatures for the two experiments and to minimize ambient temperature fluctuations, both tests (each with three repetitions) were conducted in a large insulated workshop in the summer of 2016.

References

- Weinberg, Z. G. & Ashbell, G. Engineering aspects of ensiling. *Biochem. Eng. J.* **13**, 181–188 (2003).
- Bacenet, J. & Fusi, A. The environmental burdens of maize silage production: Influence of different ensiling techniques. *Anim. Feed Sci. Tech.* **204**, 88–98 (2015).
- Wilkinson, J. M. & Davies, D. R. The aerobic stability of silage: Key findings and recent development, Review paper. *Grass Forage Sci.* **68**, 1–19 (2012).
- Pitt, R. E. & Muck, R. E. A diffusion model of aerobic deterioration at the exposed surface of bunker silo. *J. Agric. Eng. Res.* **55**, 11–26 (1993).
- Pahlow, G., Muck, R. E., Driehuis, F., Oude Elferink, S. J. W. H. & Spoelstra, S. F. Microbiology of ensiling. *Silage science and technology*. **42**, 31 (2003).
- Tabacco, E., Righi, F., Quarantelli, A. & Borreani, G. Dry matter and nutritional losses during aerobic deterioration of corn and sorghum silages as influenced by different lactic acid bacteria inocula. *J. Dairy Sci.* **94**, 1409–1419 (2011).

7. Holmes, B. J. & Muck, R. E. Packing bunkers and piles to maximize forage preservation. Sixth International Dairy Housing Conference Proceeding. *Minneapolis, St Joseph, MI, USA ASABE*. 16–18 (2007).
8. Muck, R. E. & Pitt, R. E. Aerobic deterioration in corn silage relative to silo surface. *T. ASABE*. **37**, 735–743 (1994).
9. Sun, Y. R. *et al.* Tracking oxygen and temperature dynamics in maize silage novel application of a Clack oxygen electrode. *Biosyst. Eng.* **139**, 60–65 (2015).
10. Rees, D. V. H., Audsley, E. & Neale, M. A. Apparatus for obtaining an undisturbed core of silage and for measuring the porosity and gas diffusion in the sample. *J. Agric. Eng. Res.* **28**, 107–114 (1983a).
11. Rees, D. V. H., Audsley, E. & Neale, M. A. Some physical properties that affect the rate of diffusion of oxygen into silage. *J. Agric. Sci.* **100**, 601–605 (1983b).
12. Pitt, R. E. Dry matter losses due to oxygen infiltration in silos. *J. Agric. Eng. Res.* **35**, 193–205 (1986).
13. Ruxton, G. D. & Gibson, G. J. Self-Compaction and aerobic deterioration of bunker silage: a simulation study. *J. Agric. Eng. Res.* **59**, 189–193 (1994a).
14. Ruxton, G. D. & Gibson, G. J. Effect on deterioration of spraying the open face of a silage bunker with propionic acid. *J. Agric. Eng. Res.* **58**, 159–168 (1994b).
15. Parsons, D. J. & Hoxey, R. P. A technique for measuring the permeability of silage at low pressure gradients. *J. Agric. Eng. Res.* **40**, 303–307 (1988).
16. Parsons, D. J. Modelling gas flow in a silage clamp after opening. *J. Agric. Eng. Res.* **50**, 209–218 (1991).
17. McGechan, M. B. & Williams, A. G. A model of air infiltration losses during silage storage. *J. Agric. Eng. Res.* **57**, 237–249 (1994).
18. Williams, A. G., Hoxey, R. P. & Lowe, J. F. Changes in temperature and silo gas composition during ensiling, storage and feeding-out grass silage. *Grass Forage Sci.* **52**, 176–189 (1997).
19. McEniry, J., Forristal, P. D. & O’Kiely, P. Gas composition of baled grass silage as influenced by the amount, stretch, colour and type of plastic stretch-film used to wrap the bales, and by the frequency of bale handling. *Grass Forage Sci.* **66**, 277–289 (2011).
20. Bellon-Maurel, V., Olivier Orliac, O. & Christen, P. Sensors and measurements in solid state fermentation: a review. *Process Biochem.* **38**, 881–896 (2003).
21. Jonsson, A. Growth of *Clostridium tyrobutyricum* during fermentation and aerobic deterioration of grass Silage. *J. Sci. Food Agric.* **54**, 557–568 (1991).
22. Rooke, J. A. & Hatfield, R. D. Biochemistry of Ensiling. *Silage Science and Technology*. **42**, 95–139 (2003).
23. Green, O. *et al.* Monitoring and modeling temperature variations inside silage stacks using novel wireless sensor networks. *Comput. Electron. Agr.* **69**, 149–157 (2009).
24. Diamond, L. W. & Akinfiev, N. N. Effect of changes in the pH and carbon dioxide evolution rate on the measured respiratory quotient of fermentations. *Biotechnol. Bioeng.* **40**, 1129–1138 (1992).
25. Walsberg, G. E. & Wolf, B. O. Variation in the respiratory quotient of birds and implications for indirect calorimetry using measurements of carbon dioxide. *J. Exp. Biol.* **198**, 213–219 (1995).
26. Dodds, W. S., Stutzman, L. F. & Sollami, B. J. Carbon dioxide solubility in water. *Ind. Eng. Chem.* **1**, 92–95 (1956).
27. Diamond, L. W. & Akinfiev, N. N. Solubility of CO₂ in water from –1.5 to 100 °C and from 0.1 to 100 MPa: evaluation of literature data and thermodynamic modelling. *Fluid Phase Equilib.* **208**, 265–290 (2003).
28. Duan, Z. & Sun, R. An improved model calculating CO₂ solubility in pure water and aqueous NaCl solutions from 273 to 533 K and from 0 to 2000 bar. *Chem. Geol.* **193**, 257–271 (2003).
29. Zosel, J., Oelßner, W., Decker, M., Gerlach, G. & Guth, U. The measurement of dissolved and gaseous carbon dioxide concentration. *Meas. Sci. Technol.* **22**, 1–45 (2011).
30. Uña, G. V., Romero, F. C., Goncalves, G. P. & Lorenzo, J. P. Solubility of CO₂ in Aqueous Solutions of Saccharose, Glucose, Fructose, and Glycerin. *J. Chem. Eng. Data.* **39**, 639–642 (1994).
31. Weinberg, Z. G. & Ashbell, G. *Changes in gas composition in corn silages in bunker silos during storage and feedout.* *Canadian Agr. Eng.* **36**, 155–158 (1994).
32. Zhao, Y., Wexler, A. S., Frank, H., Pan, Y. & Mitloehner, F. M. Detecting nitrous oxide in complex mixtures using FTIR spectroscopy: Silage gas. *Journal of Environmental Protection* **7**, 1719–1729 (2016).
33. Borhan, M. S., Capareda, S., Mukhtar, S., Faulkner, W. B., McGee, R. & Parnell, C. B. Jr. Determining seasonal greenhouse gas emissions from ground-level area sources in a dairy operation in central Texas. *Air & Waste Manage. Assoc.* **61**, 786–795 (2011).
34. Muck, R. E. & O’Kiely, P. Aerobic deterioration of Lucerne (*Medicago sativa*) and Maize (*Zea mais*) silages - Effects of fermentation products. *J. Sci. Food Agric.* **59**, 145–149 (1992).
35. Borreani, G. & Tabacco, E. Use of new plastic stretch films with enhanced oxygen impermeability to warp baled alfalfa silage. *T. ASABE* **53**, 635–641 (2010).
36. Shan, G. *et al.* An assessment of three different *in situ* oxygen sensors for monitoring silage production and storage. *Sensors*. **16**, 1–11 (2016).
37. Junges, D., Schmidt, P., Novinski, C. O. & Daniel, J. L. P. Additive containing homo and heterolactic bacteria on the fermentation quality of maize silage. *Acta Scientiarum. Animal Sciences.* **35**, 371–377 (2013).

Acknowledgements

We thank DFG-NSFC (Chinesische-Deutsches Zentrum fuer Wissenschaftsfoerderung) funded by Project No. GZ888, the project supported by Beijing Natural Science Foundation (No. 6164036), CLAAS Foundation for supporting our long-term cooperation in livestock farming and the Chinese Universities Scientific Fund (2017QC072). We thank Dr. G. Broil, Dr. M. Trimborn, Ms. B. Becker, Mr. W. Petriwski, Mr. W. Berchtold and Mr. R. Lutz (University of Bonn, Germany) for their great support to our experiment. We also thank Dr. Scott B. Jones (Utah State University, United States) for his valuable suggestions, who is a specialist in the China High-End Foreign Expert Recruitment Program (GDT20141100003).

Author Contributions

For this research article, M.L., G.S., H.Z., Q.C. and Y.S. conceived and designed the experiments; M.L., G.S., Y.S., Q.C., H.Z., C.M., K.H.J., W.B. and Y.F. performed the experiments; M.L., G.S., H.Z., Q.C., Y.S., A.L., D.A.G. and W.B. analyzed the data; Y.S., H.Z., M.L., K.H.J., C.M., W.B., A.L., D.M. and Z.W. contributed to the reagents/materials/analysis tools; Y.S., D.A.G., M.L. and G.S. wrote the paper.

Additional Information

Competing Interests: The authors declare that they have no competing interests.

Publisher’s note: Springer Nature remains neutral with regard to jurisdictional claims in published maps and institutional affiliations.



Open Access This article is licensed under a Creative Commons Attribution 4.0 International License, which permits use, sharing, adaptation, distribution and reproduction in any medium or format, as long as you give appropriate credit to the original author(s) and the source, provide a link to the Creative Commons license, and indicate if changes were made. The images or other third party material in this article are included in the article's Creative Commons license, unless indicated otherwise in a credit line to the material. If material is not included in the article's Creative Commons license and your intended use is not permitted by statutory regulation or exceeds the permitted use, you will need to obtain permission directly from the copyright holder. To view a copy of this license, visit <http://creativecommons.org/licenses/by/4.0/>.

© The Author(s) 2017